

THE GENERALIZED SCALAR AUXILIARY VARIABLE APPROACH (G-SAV) FOR GRADIENT FLOWS

QING CHENG*

Abstract. We establish a general framework for developing, efficient energy stable numerical schemes for gradient flows and develop three classes of generalized scalar auxiliary variable approaches (G-SAV). Numerical schemes based on the G-SAV approaches are as efficient as the original SAV schemes [30, 13] for gradient flows, i.e., only require solving linear equations with constant coefficients at each time step, can be unconditionally energy stable. But G-SAV approaches remove the definition restriction that auxiliary variables can only be square root function. The definition form of auxiliary variable is applicable to any reversible function for G-SAV approaches. Ample numerical results for phase field models are presented to validate the effectiveness and accuracy of the proposed G-SAV numerical schemes.

Key words. gradient flow, G-SAV approach, SAV approach, energy stability, phase-field

1. Introduction. Gradient flows have been widely used in science and engineering in the last few decades. Due to the second law of thermodynamics, the common characteristic of gradient flows is to satisfy the energy dissipative law in time. Correspondingly, tremendous efforts have been devoted to the construction of efficient and accurate numerical methods preserving the energy dissipative law at the discrete level for gradient flows. We refer the reader to the related review papers [17, 30, 31] and convex splitting method [19, 20, 5], stabilized method [27, 18], Average Vector Field method [9, 28], the newly developed IEQ method [33, 35], SAV method (cf. [30, 13]), Lagrange multiplier methods [21, 12], RK-SAV method [1] and gPAV method [36] which have received much attention recently due to their efficiency, flexibility and accuracy.

The key point to achieve the property of preserving energy decay for IEQ and SAV approaches lies in introducing auxiliary variables. By taking time derivative with respect to auxiliary variables, the original PDE system of gradient flows can be transformed into an equivalent form. After treating the new auxiliary variables implicitly and nonlinear terms explicitly, several classes of energy stable numerical schemes can be developed (cf. [30, 33]). But the form of the auxiliary variable is only limited to the square root function which is critical to the proof of the discrete energy stability. Meanwhile, the square root function brings inconvenience to the terms that energy can not be bounded below [14, 25]. In our new framework the square root function for auxiliary variable is not essential to devise energy stable schemes. For our G-SAV approach, the definition of scalar auxiliary variable can be any invertible function with respect to energy functional. Energy stable numerical schemes can be constructed for a large class of dissipative systems by using our generalized-SAV approach.

The goal of this paper is to establish a general framework to develop efficient and accurate time discretization for gradient flows. We propose three numerical approaches to construct schemes which enjoy all advantages of the SAV schemes, but also remove the definition restriction that auxiliary variables can only be square root function. In this paper three different G-SAV approaches will be considered: (i) in the first approach, we define the auxiliary variable as any invertible function with respect to energy functional and derive a large class of energy stable schemes which

*Department of Applied Mathematics, Illinois Institute of Technology, Chicago, IL 60616, USA (qcheng4@iit.edu).

only need to solve linear, constant coefficients equation. The small price to pay is that we need to solve a nonlinear algebraic equation whose cost is negligible. (ii) In the second approach, we treat the new auxiliary variable explicitly and derive a class of linear, no-iterative, energy stable schemes. But our numerical simulations for BCP mode [3, 4] in section 6 indicate that the first approach is more robust than the second approach, even though the second approach is much more easy to implement. (iii) In the third approach, we derive G-SAV schemes which preserve original energy dissipative law instead of modified energy. Actually the third approach is equivalent with the new Lagrange multiplier approach [12]. In summary, there are several advantages for our new three numerical approaches:

- For the first approach: the auxiliary variable can be defined by any invertible function which eliminates the constraint of free energy to be bounded below. The small price to pay is to solve a nonlinear algebraic system whose cost is negligible.
- For the second approach: by treating the auxiliary explicitly, the numerical solution and auxiliary variable can be expressed explicitly. It inherits all the advantages of the first approach, but do not need to solve a nonlinear algebraic equation at each time step. Furthermore, the auxiliary variable can be guaranteed to be positive by choosing tanh function or exponential function which IEQ and SAV approaches can not preserve. While its drawback is that it may not be robust as the first approach in dealing with models with extremely stiff terms, for example coupled Cahn-Hilliard model in Section 6.
- For the third approach: compared with IEQ and original SAV approaches, it preserves original energy dissipative law instead of modified energy. The nonlinear part of free energy do not need to be bounded from below as it is required in the SAV approach.

The remainder of this paper is structured as follows. In Section 2, we present a general framework for gradient flows by using G-SAV approach with single component. In Sections 3, we apply the G-SAV approach for gradient flows with multiple components. In Section 4, we introduce the second approach for gradient flows. In Section 5, We introduce the third approach which preserves original energy dissipative law and the technique of stabilization and adaptive time stepping strategy. In Section 6, we present several numerical simulations for Allen-Cahn and Cahn-Hilliard equations to show the validation of G-SAV schemes. Some numerical experiments will also be shown for coupled Cahn-Hilliard (BCP) model by using the first approach. Some concluding remarks are given in Section 7.

2. The first approach. We present in this section a general methodology to develop energy stable numerical schemes for gradient flows. To simplify the presentation, we consider here single-component models for gradient flows. The first generalized G-SAV approaches developed here will be extended to problems with multi-components models in the subsequent sections.

To fix the idea, we consider a system with total free energy in the form

$$(2.1) \quad E(\phi) = \int_{\Omega} \frac{1}{2} \mathcal{L}\phi \cdot \phi + F(\phi) dx,$$

where \mathcal{L} is certain linear positive operator, $F(\phi)$ is a nonlinear potential. Then a general gradient flow with the above free energy takes the following form

$$(2.2) \quad \begin{aligned} \phi_t &= -\mathcal{G}\mu, \\ \mu &= \mathcal{L}\phi + F'(\phi). \end{aligned}$$

Where \mathcal{G} is a positive operator describing the relaxation process of the system. The boundary conditions can be either one of the following two type

$$(2.3) \quad (i) \text{ periodic; or } (ii) \partial_{\mathbf{n}}\phi|_{\partial\Omega} = \partial_{\mathbf{n}}\mu|_{\partial\Omega} = 0,$$

where \mathbf{n} is the unit outward normal on the boundary $\partial\Omega$. Taking the inner products of the first two equations with μ and $-\phi_t$ respectively, taking integration by part, summing up these two results, we obtain the following energy dissipation law:

$$(2.4) \quad \frac{d}{dt}E(\phi) = -(\mathcal{G}\mu, \mu),$$

where, and in the sequel, (\cdot, \cdot) denotes the inner product in $L^2(\Omega)$. We shall also denote the L^2 -norm by $\|\cdot\|$.

Below we shall introduce the first G-SAV approach which preserves energy stability while retaining all essential advantages of the original SAV [29] approach.

2.1. The first G-SAV approach with single nonlinear potential. We rewrite the original energy (2.1) as

$$(2.5) \quad E(\phi) = \int_{\Omega} \frac{1}{2} \mathcal{L}\phi \cdot \phi d\mathbf{x} + G^{-1}\{G(\int_{\Omega} F(\phi)d\mathbf{x})\},$$

where G is an invertible function.

Firstly we define new scalar auxiliary variable $r = G(\int_{\Omega} F(\phi)d\mathbf{x})$. Taking derivative of r with respect to time, we derive

$$(2.6) \quad r_t = G'(\int_{\Omega} F(\phi)d\mathbf{x})(F'(\phi), \phi_t),$$

and notice the equality

$$(2.7) \quad (G^{-1})'\{G(\int_{\Omega} F(\phi)d\mathbf{x})\} = (G^{-1})'(r) = \frac{1}{G'(\int_{\Omega} F(\phi)d\mathbf{x})}.$$

Using two equalities (2.6)-(2.7), we shall rewrite system (2.2)

$$(2.8) \quad \partial_t\phi = -\mathcal{G}\mu,$$

$$(2.9) \quad \mu = \mathcal{L}\phi + \frac{r}{G(\int_{\Omega} F(\phi)d\mathbf{x})}F'(\phi),$$

$$(2.10) \quad \frac{d}{dt}G^{-1}(r) = (G^{-1})'(r)r_t = \frac{r}{G(\int_{\Omega} F(\phi)d\mathbf{x})}(F'(\phi), \phi_t).$$

There are various SAV approaches by choosing different functions G , for example

- The monotone polynomial SAV approach: for example $G = x^{\frac{1}{3}}, x^{\frac{1}{5}}$ or x^3 ;
- The square root SAV approach and original SAV approach [29]: $G = \sqrt{x + C}$;
- The mapped exponential SAV approach: $G = e^{\frac{x}{C}}$;
- The mapped tanh SAV approach: $G = \tanh(\frac{x}{C})$.

Where C is a positive constant. Taking the inner products of the first two equations with μ and $-\phi_t$ respectively, summing up the results along with the third equation, we obtain the following energy dissipation law:

$$(2.11) \quad \frac{d}{dt}\tilde{E}(\phi) = -(\mathcal{G}\mu, \mu),$$

where $\tilde{E}(\phi) = \int_{\Omega} \frac{1}{2} \mathcal{L}\phi \cdot \phi d\mathbf{x} + G^{-1}(r)$ is a modified energy.

2.2. Schemes based on the G-SAV approach with single nonlinear potential. A first-order numerical scheme based on the G-SAV approach for system (2.8)-(2.10) is

$$(2.12) \quad \frac{\phi^{n+1} - \phi^n}{\delta t} = -\mathcal{G}\mu^{n+1},$$

$$(2.13) \quad \mu^{n+1} = \mathcal{L}\phi^{n+1} + \frac{r^{n+1}}{G(\int_{\Omega} F(\phi^n) d\mathbf{x})} F'(\phi^n),$$

$$(2.14) \quad \frac{(G^{-1}(r))^{n+1} - (G^{-1}(r))^n}{\delta t} = \frac{r^{n+1}}{G(\int_{\Omega} F(\phi^n) d\mathbf{x})} (F'(\phi^n), \frac{\phi^{n+1} - \phi^n}{\delta t}).$$

Taking the inner products of (2.12) with μ^{n+1} and of (2.13) with $-\frac{\phi^{n+1} - \phi^n}{\delta t}$, summing up the results and taking into account (2.14), we have the following:

THEOREM 2.1. *The scheme (2.12)-(2.14) is unconditionally energy stable in the sense that*

$$\tilde{E}(\phi^{n+1}) - \tilde{E}(\phi^n) \leq -\Delta t(\mathcal{G}\mu^{n+1}, \mu^{n+1}),$$

where $\tilde{E}(\phi^k) = \int_{\Omega} \frac{1}{2} \mathcal{L}\phi^k \cdot \phi^k d\mathbf{x} + (G^{-1}(r))^k$.

Only the special case $G = x^{\frac{1}{2}}$, we can derive linear, no-iterative, original SAV schemes for system (2.26)-(2.28) in Remark 2.1. Usually scheme (2.12)-(2.14) is nonlinear and below we introduce how to solve it efficiently. Setting $\xi^{n+1} = \frac{r^{n+1}}{G(\int_{\Omega} F(\phi^n) d\mathbf{x})}$ and writing

$$(2.15) \quad \phi^{n+1} = \phi_1^{n+1} + \xi^{n+1} \phi_2^{n+1}, \quad \mu^{n+1} = \mu_1^{n+1} + \xi^{n+1} \mu_2^{n+1},$$

in the above, we find that $(\phi_i^{n+1}, \mu_i^{n+1})$ ($i = 1, 2$) can be determined as follows:

$$(2.16) \quad \frac{\phi_1^{n+1} - \phi_1^n}{\delta t} = -\mathcal{G}\mu_1^{n+1},$$

$$(2.17) \quad \mu_1^{n+1} = \mathcal{L}\phi_1^{n+1},$$

and

$$(2.18) \quad \frac{\phi_2^{n+1}}{\delta t} = -\mathcal{G}\mu_2^{n+1},$$

$$(2.19) \quad \mu_2^{n+1} = \mathcal{L}\phi_2^{n+1} + F'(\phi^n).$$

Once (ϕ_1, ϕ_2) are solved, we plug $\phi^{n+1} = \phi_1^{n+1} + \xi^{n+1} \phi_2^{n+1}$ and $r^{n+1} = \xi^{n+1} G(\int_{\Omega} F(\phi^n) d\mathbf{x})$ into equation (2.14) to obtain ξ^{n+1} by solving a nonlinear algebraic equation where Newton iterator solver with initial guess $(\xi^{n+1})^0 = 1$ should be implemented. Since ξ^{n+1} is a first-order approximation for 1. Finally solution ϕ^{n+1} can be updated by equation (2.15).

In summary, we can then determine solution ϕ^{n+1} for scheme (2.12)-(2.14) as follows:

- Solve linear constant coefficient equations (2.16) and (2.17) to obtain ϕ_1^{n+1} , equations (2.18) and (2.19) to obtain ϕ_2^{n+1} ;
- Solve ξ^{n+1} from equations (2.14) by plugging ϕ^{n+1} and r^{n+1} into it;
- Update ϕ^{n+1} from (2.15).

2.2.1. Square root SAV approach and Original SAV approach. For example, if we adopt invertible function $G = x^{\frac{1}{2}}$, then $(G^{-1}) = x^2$ and $(G^{-1})'(r)r_t = 2rr_t$, then equations (2.8)-(2.10) are reformulated as

$$(2.20) \quad \partial_t \phi = -\mathcal{G}\mu,$$

$$(2.21) \quad \mu = \mathcal{L}\phi + \frac{r}{G(\int_{\Omega} F(\phi)d\mathbf{x})} F'(\phi),$$

$$(2.22) \quad \frac{r}{G(\int_{\Omega} F(\phi)d\mathbf{x})} (F'(\phi), \phi_t) = 2rr_t = \frac{d}{dt} r^2.$$

Then, a first-order SAV scheme for the above system is

$$(2.23) \quad \frac{\phi^{n+1} - \phi^n}{\delta t} = -\mathcal{G}\mu^{n+1},$$

$$(2.24) \quad \mu^{n+1} = \mathcal{L}\phi^{n+1} + \frac{r^{n+1}}{\sqrt{\int_{\Omega} F(\phi^n)d\mathbf{x} + C_0}} F'(\phi^n),$$

$$(2.25) \quad \begin{aligned} & \frac{(r^2)^{n+1} - (r^2)^n}{\delta t} \\ &= \frac{r^{n+1}}{\sqrt{\int_{\Omega} F(\phi^n)d\mathbf{x} + C_0}} (F'(\phi^n), \frac{\phi^{n+1} - \phi^n}{\delta t}). \end{aligned}$$

Taking the inner products of (2.23) with μ^{n+1} and of (2.24) with $-\frac{\phi^{n+1} - \phi^n}{\delta t}$, summing up the results and taking into account (2.25), we have the following:

THEOREM 2.2. *The scheme (2.23)-(2.25) is unconditionally energy stable in the sense that*

$$\tilde{E}(\phi^{n+1}) - \tilde{E}(\phi^n) \leq -\Delta t (\mathcal{G}\mu^{n+1}, \mu^{n+1}),$$

where $\tilde{E}(\phi^k) = \int_{\Omega} \frac{1}{2} \mathcal{L}\phi^k \cdot \phi^k d\mathbf{x} + (r^k)^2$.

Remark 2.1. *If we can cancel r on both sides from equation (2.22) and obtain*

$$(2.26) \quad \partial_t \phi = -\mathcal{G}\mu,$$

$$(2.27) \quad \mu = \mathcal{L}\phi + \frac{r}{G(\int_{\Omega} F(\phi)d\mathbf{x})} F'(\phi),$$

$$(2.28) \quad r_t = \frac{1}{2} \frac{1}{G(\int_{\Omega} F(\phi)d\mathbf{x})} (F'(\phi), \phi_t).$$

Notice that $G = x^{\frac{1}{2}}$, then it is observed that the system (2.26)-(2.28) is exactly the original SAV approach in [30, 29]. By treating r implicitly, a large class of linear numerical schemes have been proposed in [30, 29, 14, 24].

2.2.2. The mapped tanh SAV approach. In order to make $r = \tanh(\int_{\Omega} F(\phi)d\mathbf{x})$ not too close to ± 1 numerically since $\tanh^{-1}(r = \pm 1) \rightarrow \infty$. Then we consider a mapped function $G = \tanh(\frac{x}{C})$, then $G^{-1} = C \tanh^{-1}(x)$, and C is a large positive constant. We define a new variable $r = \tanh(\frac{\int_{\Omega} F(\phi)d\mathbf{x}}{C})$, then equations (2.8)-(2.10)

are reformulated as

$$(2.29) \quad \partial_t \phi = -\mathcal{G}\mu,$$

$$(2.30) \quad \mu = \mathcal{L}\phi + \frac{r}{\tanh(\frac{\int_{\Omega} F(\phi) d\mathbf{x}}{C})} F'(\phi),$$

$$(2.31) \quad \frac{d}{dt}(C \tanh^{-1}(r)) = \frac{r}{\tanh(\frac{\int_{\Omega} F(\phi) d\mathbf{x}}{C})} (F'(\phi), \phi_t).$$

Then, a first-order SAV scheme for the above system is

$$(2.32) \quad \frac{\phi^{n+1} - \phi^n}{\delta t} = -\mathcal{G}\mu^{n+1},$$

$$(2.33) \quad \mu^{n+1} = \mathcal{L}\phi^{n+1} + \frac{r^{n+1}}{\tanh(\frac{\int_{\Omega} F(\phi^n) d\mathbf{x}}{C})} F'(\phi^n),$$

$$(2.34) \quad \frac{(C \tanh^{-1}(r))^{n+1} - (C \tanh^{-1}(r))^n}{\delta t} = \frac{r^{n+1}}{\tanh(\frac{\int_{\Omega} F(\phi^n) d\mathbf{x}}{C})} (F'(\phi^n), \frac{\phi^{n+1} - \phi^n}{\delta t}).$$

Remark 2.2. The tanh-SAV scheme (2.32)-(2.34) takes a big advantage of dealing with nonlinear potential $F(\phi^n)$ which is not bounded up and below or the singular potential. For example the logarithmic (singular) functions: $F = \alpha\phi + \beta\ln(\frac{1+\phi}{1-\phi})$, $F = \phi + (1-\phi)\log(1-\phi)$ [23, 15] and MBE model without slope selection [14]. Because the domain of function tanh is $(-\infty, \infty)$ while the range is $(-1, 1)$.

Taking the inner products of (2.32) with μ^{n+1} and of (2.33) with $-\frac{\phi^{n+1} - \phi^n}{\delta t}$, summing up the results and taking into account (2.34), we have the following:

THEOREM 2.3. The scheme (2.32)-(2.34) is unconditionally energy stable in the sense that

$$\tilde{E}(\phi^{n+1}) - \tilde{E}(\phi^n) \leq -\Delta t (\mathcal{G}\mu^{n+1}, \mu^{n+1}),$$

where $\tilde{E}(\phi^k) = \int_{\Omega} \frac{1}{2} \mathcal{L}\phi^k \cdot \phi^k d\mathbf{x} + (\tanh^{-1}(r))^k$.

2.3. Schemes based on the MG-SAV approach with multiple nonlinear potentials. If we consider gradient flows with multiple nonlinear potentials, where the total free energy is

$$(2.35) \quad E(\phi) = \int_{\Omega} \frac{1}{2} \mathcal{L}\phi \cdot \phi + \sum_{i=1}^m F_i(\phi) d\mathbf{x},$$

then the multiple generalized scalar auxiliary variable approach (MG-SAV) may achieve better accuracy for numerical simulation which has been observed in [13]. The gradient flow with multiple nonlinear potentials is formulated as the following form

$$(2.36) \quad \begin{aligned} \phi_t &= -\mathcal{G}\mu, \\ \mu &= \mathcal{L}\phi + \sum_{i=1}^m F'_i(\phi), \end{aligned}$$

where $F'_i(\phi)$ is the variational derivative of F_i . By using the MG-SAV approach, we can also rewrite the energy (2.35) as

$$(2.37) \quad E(\phi) = \int_{\Omega} \frac{1}{2} \mathcal{L}\phi \cdot \phi d\mathbf{x} + \sum_{i=1}^m G_i^{-1} \{G_i(\int_{\Omega} F_i(\phi) d\mathbf{x})\},$$

where G_i are various invertible functions for $i = 1, 2, \dots, m$. Setting new variables to be

$$(2.38) \quad r_i = G_i(\int_{\Omega} F_i(\phi) d\mathbf{x}).$$

Now we shall derive an equivalent form

$$(2.39) \quad \partial_t \phi = -\mathcal{G}\mu,$$

$$(2.40) \quad \mu = \mathcal{L}\phi + \sum_{i=1}^m \frac{r_i}{G_i(\int_{\Omega} F_i(\phi) d\mathbf{x})} F'_i(\phi),$$

$$(2.41) \quad \frac{d}{dt} G_i^{-1}(r_i) = \frac{r_i}{G_i(\int_{\Omega} F_i(\phi) d\mathbf{x})} (F'_i(\phi), \phi_t).$$

Then a second-order BDF2 scheme can be constructed for equations (2.39)-(2.41)

$$(2.42) \quad \frac{3\phi^{n+1} - 4\phi^n + \phi^{n-1}}{2\delta t} = -\mathcal{G}\mu^{n+1},$$

$$(2.43) \quad \mu^{n+1} = \mathcal{L}\phi^{n+1} + \sum_{i=1}^m \frac{r_i^{n+1}}{G_i(\int_{\Omega} F_i(\phi^{\dagger,n}) d\mathbf{x})} F'_i(\phi^{\dagger,n}),$$

$$(2.44) \quad \frac{3G_i^{-1}(r_i^{n+1}) - 4G_i^{-1}(r_i^n) + G_i^{-1}(r_i^{n-1})}{2\delta t} = \frac{r_i^{n+1}}{G_i(\int_{\Omega} F_i(\phi^{\dagger,n}) d\mathbf{x})} (F'_i(\phi^{\dagger,n}), \frac{3\phi^{n+1} - 4\phi^n + \phi^{n-1}}{2\delta t}).$$

Where G_i with $i = 1, 2, \dots, m$ are invertible functions and $g^{\dagger,n} = 2g^n - g^{n-1}$ for any sequence $\{g^n\}$.

Taking inner product of equation (2.42) with μ^{n+1} , of equation (2.43) with $\frac{3\phi^{n+1} - 4\phi^n + \phi^{n-1}}{2\delta t}$ and combining with equations (2.44), we derive the following energy dissipative law for scheme (2.42)-(2.44).

THEOREM 2.4. *The scheme (2.42)-(2.44) is unconditionally energy stable in the sense that*

$$\tilde{E}(\phi^{n+1}) - \tilde{E}(\phi^n) \leq -\delta t (\mathcal{G}\mu^{n+1}, \mu^{n+1}),$$

where $\tilde{E}(\phi^k) = \int_{\Omega} \frac{1}{4} (\mathcal{L}\phi^k \cdot \phi^k + \mathcal{L}(2\phi^k - \phi^{k-1}) \cdot (2\phi^k - \phi^{k-1})) d\mathbf{x} + \sum_{i=1}^m (\frac{3}{2} G_i^{-1}(r_i^k) - \frac{1}{2} G_i^{-1}(r_i^{k-1}))$.

Below we show how to solve the scheme (2.42)-(2.44). Define new variables

$$(2.45) \quad \xi_i^{n+1} = \frac{r_i^{n+1}}{G_i(\int_{\Omega} F_i(\phi^{\dagger,n}) d\mathbf{x})},$$

for $i = 1, 2, \dots, m$, then ϕ^{n+1} and μ^{n+1} can be expressed as

$$(2.46) \quad \phi^{n+1} = \phi_1^{n+1} + \sum_{i=1}^m \xi_i^{n+1} \phi_{i,2}^{n+1},$$

and

$$(2.47) \quad \mu^{n+1} = \mu_1^{n+1} + \sum_{i=1}^m \xi_i^{n+1} \mu_{i,2}^{n+1}.$$

Where $(\phi_1^{n+1}, \mu_1^{n+1})$ and $(\phi_{i,2}^{n+1}, \mu_{i,2}^{n+1})$ can be determined as follows:

$$(2.48) \quad \frac{3\phi_1^{n+1} - 4\phi_1^n + \phi_1^{n-1}}{2\delta t} = -\mathcal{G}\mu_1^{n+1},$$

$$(2.49) \quad \mu_1^{n+1} = \mathcal{L}\phi_1^{n+1},$$

and

$$(2.50) \quad \frac{3\phi_{i,2}^{n+1} - 4\phi_{i,2}^n + \phi_{i,2}^{n-1}}{2\delta t} = -\mathcal{G}\mu_{i,2}^{n+1},$$

$$(2.51) \quad \mu_{i,2}^{n+1} = \mathcal{L}\phi_{i,2}^{n+1} + F'_i(\phi_i^{\dagger,n}).$$

Once $(\phi_1^{n+1}, \mu_1^{n+1})$ and $(\phi_{i,2}^{n+1}, \mu_{i,2}^{n+1})$ are known, we plug equations (2.45) and (2.46) into equations (2.44) to obtain a coupled $m \times m$ nonlinear algebraic system of ξ_i^{n+1} for $i = 1, 2, \dots, m$. Finally, we update ϕ^{n+1} from (2.46).

In summary, we can then determine solution ϕ^{n+1} for scheme (2.42)-(2.44) as follows:

- Solve linear constant coefficient equation from equation (2.48) and equation (2.49) to obtain ϕ_1^{n+1} , equation (2.50) and equation (2.51) to obtain $\phi_{i,2}^{n+1}$;
- Solve ξ_i^{n+1} for $i = 1, 2, \dots, m$ from equation (2.44) by plugging equations (2.45) and (2.46) into it;
- Update ϕ^{n+1} from (2.46).

3. Schemes based on the G-SAV approach with multiple components.

In this section, we consider multiple-components phase field models which play an important role in describing three material components [6, 34]. We introduce ϕ_i ($i = 1, 2, \dots, m$) be the i -th phase variables. A special form of total free energy for multi-phase system is formulated as

$$(3.1) \quad E(\phi_1, \phi_2, \dots, \phi_m) = \sum_{i,j=1}^m \int_{\Omega} \mathcal{L}\phi_i \cdot \phi_j d\mathbf{x} + \int_{\Omega} F(\phi_1, \phi_2, \dots, \phi_m) d\mathbf{x},$$

where \mathcal{L} is a self-adjoint nonnegative linear operator, and the constant matrix d_{ij} is symmetric positive definite. $F(\phi_1, \phi_2, \dots, \phi_m)$ is nonlinear potential. We derive the multi-components phase field model by taking variational derivative with respect to (3.1),

$$(3.2) \quad \begin{aligned} \partial_t \phi_i &= M\mathcal{G}\mu_i, \quad i = 1, 2, \dots, m \\ \mu_i &= \mathcal{L}\phi_i + f_i, \end{aligned}$$

with some suitable boundary condition, M is mobility constant.

THEOREM 3.1. *The multi-components phase field equation (3.2) satisfies the following energy dissipative law:*

$$(3.3) \quad \frac{d}{dt} E(\phi_1, \phi_2, \dots, \phi_m) = -M \sum_{i=1}^m (\mathcal{G}\mu_i, \mu_i).$$

Proof. Taking inner product of equation (3.2) with μ_i and $\partial_t \phi_i$ respectively for $i = 1, 2, \dots, m$, taking integration by parts and summing up these three equalities. The desired energy dissipative law is obtained. \square

We rewrite energy (3.1) to the following form

$$(3.4) \quad E(\phi_1, \phi_2, \dots, \phi_m) = \sum_{i=1}^m \int_{\Omega} \mathcal{L}\phi_i \cdot \phi_i d\mathbf{x} + G^{-1} \left\{ G \left(\int_{\Omega} F(\phi_1, \phi_2, \dots, \phi_m) d\mathbf{x} \right) \right\}.$$

Introducing a new SAV

$$(3.5) \quad r(t) = G \left(\int_{\Omega} F(\phi_1, \phi_2, \dots, \phi_m) d\mathbf{x} \right),$$

then the system (3.2) is reformulated to be

$$(3.6) \quad \begin{aligned} \partial_t \phi_i &= M \mathcal{G}\mu_i, \quad i = 1, 2, \dots, m \\ \mu_i &= \mathcal{L}\phi_i + \frac{r}{G \left(\int_{\Omega} F(\phi_1, \phi_2, \dots, \phi_m) d\mathbf{x} \right)} f_i, \\ \frac{d}{dt} G^{-1}(r) &= \frac{r}{G \left(\int_{\Omega} F(\phi_1, \phi_2, \dots, \phi_m) d\mathbf{x} \right)} \sum_{i=1}^3 (f_i, \partial_t \phi_i). \end{aligned}$$

Then an iterative Crank-Nicolson scheme for system (3.6) is

$$(3.7) \quad \begin{aligned} \frac{\phi_i^{n+1} - \phi_i^n}{\delta t} &= M \mathcal{G}\mu_i^{n+\frac{1}{2}}, \quad i = 1, 2, 3, \\ \mu_i^{n+\frac{1}{2}} &= \mathcal{L}\phi_i^{n+\frac{1}{2}} + \frac{r^{n+\frac{1}{2}}}{G \left(\int_{\Omega} F(\phi_1^{*,n}, \phi_2^{*,n}, \dots, \phi_m^{*,n}) d\mathbf{x} \right)} f_i^{*,n}, \\ \frac{(G^{-1}(r))^{n+1} - (G^{-1}(r))^n}{\delta t} &= \frac{r^{n+\frac{1}{2}}}{G \left(\int_{\Omega} F(\phi_1^{*,n}, \phi_2^{*,n}, \phi_3^{*,n}) d\mathbf{x} \right)} \sum_{i=1}^3 \left(f_i^{*,n}, \frac{\phi_i^{n+1} - \phi_i^n}{\delta t} \right), \end{aligned}$$

where $f_i^{*,n} = \frac{1}{2}(3f_i^n - f_i^{n-1})$ and $\phi^{*,n} = \frac{1}{2}(3\phi^n - \phi^{n-1})$. It is easy to see that a non-iterative Crank-Nicolson scheme can be developed similarly by treating r explicitly. And it can also be solved efficiently as one component case.

Taking inner product of equation (3.7) with $\mu_i^{n+\frac{1}{2}}$, $\frac{\phi_i^{n+1} - \phi_i^n}{\delta t}$ for $i = 1, 2, 3$, summing up these three equalities and combining the third equation of (3.7), we derive the following energy dissipative law for scheme (3.7).

THEOREM 3.2. *The scheme (3.7)- is unconditionally energy stable in the sense that*

$$\tilde{E}(\phi_1^{n+1}, \phi_2^{n+1}, \dots, \phi_m^{n+1}) - \tilde{E}(\phi_1^n, \phi_2^n, \dots, \phi_m^n) \leq -M \sum_{i=1}^m (\mathcal{G}\mu_i^{n+\frac{1}{2}}, \mu_i^{n+\frac{1}{2}}),$$

where $\tilde{E}(\phi^k) = \int_{\Omega} \sum_{i=1}^m \frac{1}{2} \mathcal{L}\phi_i^k \cdot \phi_i^k d\mathbf{x} + G^{-1}(r^k)$.

The numerical scheme (3.7) can also be efficiently solved. Setting

$$\xi^{n+\frac{1}{2}} = \frac{r^{n+\frac{1}{2}}}{G(\int_{\Omega} F(\phi_1^{*,n}, \phi_2^{*,n}, \dots, \phi_m^{*,n}) d\mathbf{x})}.$$

Obviously $\xi^{n+\frac{1}{2}}$ is a second-order approximation for 1. writing

$$(3.8) \quad \phi_i^{n+1} = \phi_{i,1}^{n+1} + \xi^{n+\frac{1}{2}} \phi_{i,2}^{n+1}, \quad \mu_i^{n+1} = \mu_{i,1}^{n+1} + \xi^{n+\frac{1}{2}} \mu_{i,2}^{n+1},$$

in the above, we find that $(\phi_i^{n+1}, \mu_i^{n+1})$ ($i = 1, 2, \dots, m$) can be determined as follows:

$$(3.9) \quad \frac{\phi_{i,1}^{n+1} - \phi_i^n}{\delta t} = M\mathcal{G}\mu_{i,1}^{n+\frac{1}{2}},$$

$$(3.10) \quad \mu_{i,1}^{n+\frac{1}{2}} = \mathcal{L}\phi_{i,1}^{n+\frac{1}{2}},$$

and

$$(3.11) \quad \frac{\phi_{i,2}^{n+1}}{\delta t} = M\mathcal{G}\mu_{i,2}^{n+\frac{1}{2}},$$

$$(3.12) \quad \mu_{i,2}^{n+\frac{1}{2}} = \mathcal{L}\phi_{i,2}^{n+\frac{1}{2}} + f_i^{*,n}.$$

Once $(\phi_{i,1}^{n+1}, \phi_{i,2}^{n+1})$ are solved, we plug $\phi_i^{n+1} = \phi_{i,1}^{n+1} + \xi^{n+\frac{1}{2}} \phi_{i,2}^{n+1}$ and

$$(3.13) \quad r^{n+\frac{1}{2}} = \xi^{n+\frac{1}{2}} G(\int_{\Omega} F(\phi_1^{*,n}, \phi_2^{*,n}, \dots, \phi_m^{*,n}) d\mathbf{x}),$$

into the third equation of (3.7) to obtain $\xi^{n+\frac{1}{2}}$ by solving a nonlinear algebraic equation where Newton iterator solver should be implemented with initial guess $(\xi^{n+\frac{1}{2}})^0 = 1$. Finally solution ϕ^{n+1} can be updated by equation (3.8).

In summary, we can then determine solution ϕ_i^{n+1} for $i = 1, 2, \dots, m$ as follows:

- Solve linear constant coefficient equation from equations (3.9)-(3.10) to obtain $\phi_{i,1}^{n+1}$ and equations (3.11)-(3.12) to obtain $\phi_{i,2}^{n+1}$;
- Solve $\xi^{n+\frac{1}{2}}$ from the third equation (3.7) by plugging equation (3.13) into it;
- Update $\phi_i^{n+1} = \phi_{i,1}^{n+1} + \xi^{n+\frac{1}{2}} \phi_{i,2}^{n+1}$ for $i = 1, 2, \dots, m$.

Hence, the above scheme can be implemented very efficiently.

4. The second approach. We can treat scalar variable r explicitly in equation (2.9), and derive an no-iterative, first-order numerical scheme of G-SAV for system (2.8)-(2.10) is

$$(4.1) \quad \frac{\phi^{n+1} - \phi^n}{\delta t} = -\mathcal{G}\mu^{n+1},$$

$$(4.2) \quad \mu^{n+1} = \mathcal{L}\phi^{n+1} + \frac{r^n}{G(\int_{\Omega} F(\phi^n) d\mathbf{x})} F'(\phi^n),$$

$$(4.3) \quad \frac{(G^{-1}(r))^{n+1} - (G^{-1}(r))^n}{\delta t} = \frac{r^n}{G(\int_{\Omega} F(\phi^n) d\mathbf{x})} (F'(\phi^n), \frac{\phi^{n+1} - \phi^n}{\delta t}).$$

Taking the inner products of (4.1) with μ^{n+1} and of (4.2) with $-\frac{\phi^{n+1} - \phi^n}{\delta t}$, summing up the results and taking into account (4.3), we have the following:

THEOREM 4.1. *The scheme (4.1)-(4.3) is unconditionally energy stable in the sense that*

$$\tilde{E}(\phi^{n+1}) - \tilde{E}(\phi^n) \leq -\Delta t(\mathcal{G}\mu^{n+1}, \mu^{n+1}),$$

where $\tilde{E}(\phi^k) = \int_{\Omega} \frac{1}{2} \mathcal{L}\phi^k \cdot \phi^k d\mathbf{x} + (G^{-1}(r))^k$.

We now show that the above G-SAV scheme (4.1)-(4.3) can be efficiently implemented. Writing equation (4.1) as

$$(4.4) \quad \frac{\phi^{n+1}}{\delta t} + \mathcal{G}\mathcal{L}\phi^{n+1} = \frac{\phi^n}{\delta t} - \mathcal{G}\left\{\frac{r^n}{G(\int_{\Omega} F(\phi^n) d\mathbf{x})} F'(\phi^n)\right\}.$$

Defining Linear operator $\chi = \frac{1}{\delta t} + \mathcal{G}\mathcal{L}$, then ϕ^{n+1} can be solved by

$$(4.5) \quad \phi^{n+1} = \chi^{-1}\left\{\frac{\phi^n}{\delta t} - \mathcal{G}\left\{\frac{r^n}{G(\int_{\Omega} F(\phi^n) d\mathbf{x})} F'(\phi^n)\right\}\right\}.$$

r^{n+1} can be updated by plugging ϕ^{n+1} into equation (4.3)

$$(4.6) \quad (G^{-1}(r))^{n+1} = (G^{-1}(r))^n + \delta t \frac{r^n}{G(\int_{\Omega} F(\phi^n) d\mathbf{x})} (F'(\phi^n), \frac{\phi^{n+1} - \phi^n}{\delta t}).$$

Finally $r^{n+1} = G(G^{-1}(r))^{n+1}$.

In summary, we can then determine solution ϕ^{n+1} as follows:

- Solve a linear constant coefficient equation from (4.5);
- Update $(G^{-1}(r))^{n+1}$ from equation (4.6);
- Obtain $r^{n+1} = G(G^{-1}(r))^{n+1}$.

Hence, the above scheme can be implemented very efficiently. The second-order numerical schemes based on BDF2 or Crank-Nicolson can be constructed similarly.

Remark 4.1. *If we choose function $G = e^x$ as the exponential function, which is the just so-called E-SAV approach developed in [26], some numerical simulations are also presented in [26] to validate the efficiency of this approach.*

5. The third approach (Lagrange multiplier approach). Both the first and second approaches preserve modified energy dissipative law in discrete level. In this section, we develop SAV approach which preserves original energy dissipative law instead of modified energy dissipative law. Since the auxiliary variable is defined as $r = G(\int_{\Omega} F(\phi) d\mathbf{x})$, then we obtain $\int_{\Omega} F(\phi) d\mathbf{x} = G^{-1}(r)$. The system (2.2) can be reformulated as

$$(5.1) \quad \partial_t \phi = -\mathcal{G}\mu,$$

$$(5.2) \quad \mu = \mathcal{L}\phi + \frac{r}{G(\int_{\Omega} F(\phi) d\mathbf{x})} F'(\phi),$$

$$(5.3) \quad \frac{d}{dt} \int_{\Omega} F(\phi) d\mathbf{x} = \frac{d}{dt} G^{-1}(r) = \frac{r}{G(\int_{\Omega} F(\phi) d\mathbf{x})} (F'(\phi), \phi_t).$$

A second-order scheme for (5.1)-(5.3) is constructed as

$$(5.4) \quad \frac{3\phi^{n+1} - 4\phi^n + \phi^{n-1}}{2\delta t} = -\mathcal{G}\mu^{n+1},$$

$$(5.5) \quad \mu^{n+1} = \mathcal{L}\phi^{n+1} + \frac{r^{n+1}}{G(\int_{\Omega} F(\phi^{\dagger,n})d\mathbf{x})} F'(\phi^{\dagger,n}),$$

$$\frac{\int_{\Omega} 3F(\phi^{n+1}) - 4F(\phi^n) + F(\phi^{n-1})d\mathbf{x}}{2\delta t}$$

$$(5.6) \quad = \frac{r^{n+1}}{G(\int_{\Omega} F(\phi^{\dagger,n})d\mathbf{x})} (F'(\phi^{\dagger,n}), \frac{3\phi^{n+1} - 4\phi^n + \phi^{n-1}}{2\delta t}).$$

Taking the inner products of (5.4) with μ^{n+1} and of (5.5) with $-\frac{3\phi^{n+1} - 4\phi^n + \phi^{n-1}}{2\delta t}$, summing up the results and taking into account (5.6), we have the following:

THEOREM 5.1. *The scheme (5.4)-(5.6) is unconditionally energy stable in the sense that*

$$\tilde{E}(\phi^{n+1}) - \tilde{E}(\phi^n) \leq -\Delta t(\mathcal{G}\mu^{n+1}, \mu^{n+1}),$$

where $\tilde{E}(\phi^k) = \int_{\Omega} \frac{1}{4}(\mathcal{L}\phi^k \cdot \phi^k + \mathcal{L}(2\phi^k - \phi^{k-1}) \cdot (2\phi^k - \phi^{k-1}))d\mathbf{x} + \frac{3}{2} \int_{\Omega} F(\phi^k)d\mathbf{x} - \frac{1}{2} \int_{\Omega} F(\phi^k)d\mathbf{x}$.

Remark 5.1. *From Theorem 5.1 we find that scheme (5.4)-(5.6) satisfies original energy dissipative law. It is also observed that the scheme (5.4)-(5.6) is exactly the same with the Lagrange multiplier approach [12] by treating*

$$\eta^{n+1} = \frac{r^{n+1}}{G(\int_{\Omega} F(\phi^{\dagger,n})d\mathbf{x})}.$$

Ample numerical simulations are shown in [12] to validate the efficiency of Lagrange multiplier approach.

5.1. Stabilized-G-SAV approach and adaptive time stepping. For problems with stiff nonlinear terms, one may have to use very small time steps to obtain accurate results with G-SAV above. In order to allow larger time steps while achieving desired accuracy, we may add suitable stabilization and use adaptive time stepping.

5.1.1. Stabilization. Instead of solving (2.2), we consider a perturbed system with two additional stabilization terms

$$(5.7) \quad \begin{aligned} \phi_t &= -\mathcal{G}\mu, \\ \mu &= \mathcal{L}\phi + \epsilon_1\phi_{tt} + \epsilon_2\mathcal{L}\phi_{tt} + F'(\phi), \end{aligned}$$

where ϵ_i , $i = 1, 2$ are two small stabilization constants whose choices will depend on how stiff are the nonlinear terms. It is easy to see that the above system is a gradient flow with a perturbed free energy $E_{\epsilon}(\phi) = E(\phi) + \frac{\epsilon_1}{2}(\phi_t, \phi_t) + \frac{\epsilon_2}{2}(\mathcal{L}\phi_t, \phi_t)$ and satisfies the following energy law:

$$(5.8) \quad \frac{d}{dt}E_{\epsilon}(\phi) = -(\mathcal{G}\mu, \mu).$$

The schemes presented before for (2.2) can all be easily extended for (5.7) while keeping the same simplicity. For example, a second order scheme based on the second

approach is:

$$(5.9) \quad \frac{\phi^{n+1} - \phi^n}{\delta t} = -\mathcal{G}\mu^{n+1/2},$$

$$\mu^{n+1/2} = \mathcal{L}\phi^{n+1/2} + \frac{\epsilon_1}{(\delta t)^2}(\phi^{n+1} - 2\phi^n + \phi^{n-1})$$

$$(5.10) \quad + \frac{\epsilon_2}{(\delta t)^2}\mathcal{L}(\phi^{n+1} - 2\phi^n + \phi^{n-1}) + \frac{r^{n+\frac{1}{2}}}{G(\int_{\Omega} F(\phi^{*,n})d\mathbf{x})}F'(\phi^{*,n}),$$

$$(5.11) \quad \frac{G^{-1}(r^{n+1}) - G^{-1}(r^n)}{\delta t} = \frac{r^{n+\frac{1}{2}}}{G(\int_{\Omega} F(\phi^{*,n})d\mathbf{x})}(F'(\phi^{*,n}), \frac{\phi^{n+1} - \phi^n}{\delta t}),$$

where $f^{n+1/2} = \frac{1}{2}(f^{n+1} + f^n)$ and $f^{*,n} = \frac{1}{2}(3f^n - f^{n-1})$ for any sequence $\{f^n\}$.

Taking the inner products of (5.9) with $\mu^{n+1/2}$ and of (5.10) with $-\frac{\phi^{n+1}-\phi^n}{\delta t}$, summing up the results along with (5.11) and dropping some unnecessary terms, we immediately derive the following results:

THEOREM 5.2. *The scheme (5.9)-(5.11) is unconditionally energy stable in the sense that*

$$E_{\epsilon}^{n+1} - E_{\epsilon}^n \leq -\delta t(\mathcal{G}\mu^{n+1/2}, \mu^{n+1/2}),$$

where $E_{\epsilon}^k = E(\phi^k) + \frac{\epsilon_1}{2}(\frac{\phi^k - \phi^{k-1}}{\delta t}, \frac{\phi^k - \phi^{k-1}}{\delta t}) + \frac{\epsilon_2}{2}(\mathcal{L}\frac{\phi^k - \phi^{k-1}}{\delta t}, \frac{\phi^k - \phi^{k-1}}{\delta t})$ with $E(\phi)$ being the original free energy defined in (2.1).

It is clear that the above scheme can be efficiently implemented as the scheme (2.12)-(2.14).

5.1.2. Adaptive time stepping. To improve the efficiency of G-SAV approach, one can combine them with an adaptive time stepping method. Many numerical examples have been provided for the original SAV approaches [13, 29, 12]. Similarly, we can also apply an adaptive time stepping strategy for G-SAV approach since all the schemes using G-SAV are energy stable. For example, we can combine an adaptive time stepping method with G-SAV scheme (5.9)-(5.11) and achieve a second-order adaptive Cank-Nicolson scheme, see [13].

6. Numerical results. In this section some numerical experiments will be provided to validate their stability and convergence rates for the first and second G-SAV approaches, since enough numerical simulations are shown in [12] for the third approach. We will compare the performance of different G-SAV approaches by choosing various function G . In all numerical examples below, we assume periodic boundary conditions and use a Fourier Spectral method in space. The default computational domain is $[-\pi, \pi]^d$ with $d = 2$.

6.1. Validation and comparison. We consider famous Allen-cahn [2] and Cahn-Hilliard [7, 8] equations and use 128 modes in each direction in our Fourier Spectral method so that the spatial discretization errors are negligible compared with time discretization error. The total free energy of Allen-Cahn and Cahn-Hilliard equation is

$$E_{tot} = \int_{\Omega} \frac{1}{2}|\nabla\phi|^2 + F(\phi)d\mathbf{x},$$

where $F(\phi) = \frac{1}{4\epsilon^2}(\phi^2 - 1)^2$ is double well potential. The form of chemical potential in (2.2) is

$$\mu = -\Delta\phi + F'(\phi),$$

the $\mathcal{G} = I$ for Allen-Cahn equation and $\mathcal{G} = \Delta$ for Cahn-Hilliard equation.

6.1.1. Comparison of various G-SAV approaches. We first investigate the performance of various G-SAV approaches proposed in Section 2. We consider the 2D Cahn-Hilliard equation and choose a random initial condition

$$(6.1) \quad \phi(x, y) = 0.03 + 0.001 \text{rand}(x, y),$$

where $\text{rand}(x, y)$ represents random data between $[-1, 1]^2$.

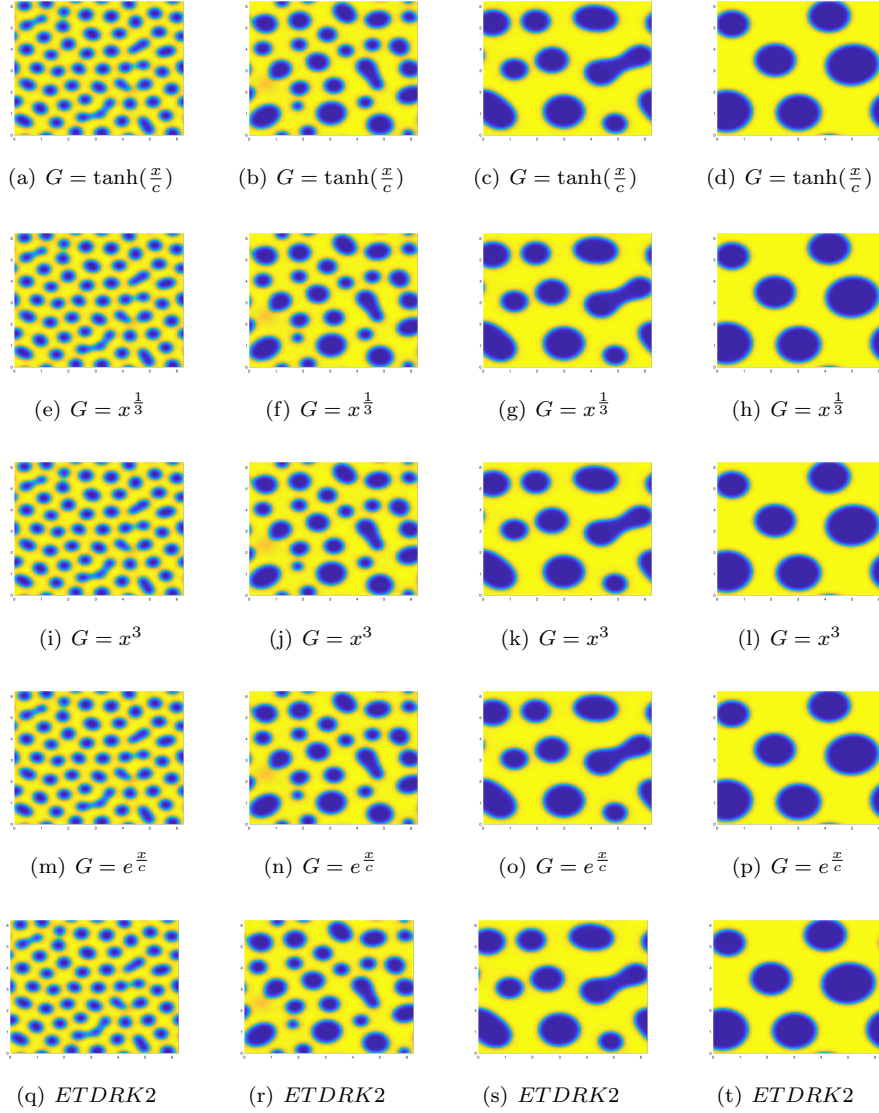


FIG. 1. The 2D dynamical evolutions of the phase variable ϕ at $t = 0.0025, 0.01, 0.04, 0.1$ for the Cahn-Hilliard equation with parameters $\epsilon^2 = 0.005$ computed by BDF2 scheme of various non-iterative SAV approaches and ETDRK2 with $\delta t = 10^{-5}$. The constant c is equal to 10^4 for \tanh and mapped exponential SAV approaches.

In the Fig. 1, we plot the dynamic evolution of phase separation for Cahn-Hilliard equation by using different BDF2 schemes of the first approach with $\delta t = 10^{-5}$ and

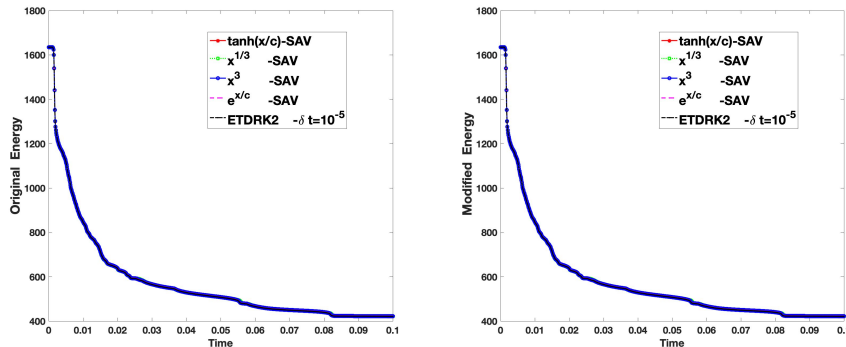


FIG. 2. Left: Evolutions of original energy by using various SAV approaches and ETDRK2 for Fig. 1; Right: Evolutions of the corresponding modified energy of various SAV approaches.

scheme ETDRK2 [16] with $\delta t = 10^{-5}$. We observe that all the G-SAV of first approach and ETDRK2 approaches lead to indistinguishable ϕ in Fig. 1. This indicates that the accuracy of BDF2 schemes by using G-SAV approaches is comparable with ETDRK2.

In the Fig. 2, the evolutions of original and modified energy computed by schemes G-SAV and ETDRK2 are depicted. From this figure we find no visible difference are observed for those energy curves which are consistent with the numerical results in Fig. 1.

6.1.2. Convergence rate with given exact solution. We test the convergence rate of BDF2 and Crank-Nicolson schemes using various G-SAV approaches for 2D Allen-Cahn equation with the exact solution

$$(6.2) \quad \phi(x, y, t) = \left(\frac{\sin(2x) \cos(2y)}{4} + 0.48 \right) \left(1 - \frac{\sin^2(t)}{2} \right).$$

The manufactured exact solution (6.2) are obtained by adding a force term $f(\mathbf{x}, t)$ into Allen-Cahn equation. In table 1 and table 2, we show the L^∞ errors of ϕ between numerical solution and the given exact solution with different time steps which are computed by BDF2 and Crank-Nicolson schemes of the first approach with $G = \tanh(\frac{x}{c})$ and $G = x^3$, where the constant $c = 10^4$. Similar with table 1 and table 2, we show the the L^∞ errors of ϕ between numerical solution and the given exact solution by using the second approach with same functions G in table 3 and table 4. We observe that both first and second approaches obtain second-order convergence rates in time.

6.1.3. Cahn-Hilliard equation with singular potential. In this subsection, we show the validation for Cahn-Hilliard equation with logarithmic (singular) potential [11]. The total free energy is

$$(6.3) \quad E(\phi) = \int_{\Omega} \frac{\epsilon^2}{2} |\nabla \phi|^2 + F(\phi) d\mathbf{x},$$

where the logarithmic Flory Huggins energy potential is

$$(6.4) \quad F(\phi) = -\frac{\theta}{2} \phi^2 + (1 + \phi) \ln(1 + \phi) + (1 - \phi) \ln(1 - \phi).$$

δt	$BDF2 - \tanh(\frac{x}{c})$	Order	$CN2 - \tanh(\frac{x}{c})$	Order
8×10^{-4}	$5.41E(-4)$	–	$5.77E(-4)$	–
4×10^{-4}	$1.35E(-4)$	1.98	$1.46E(-4)$	2.00
2×10^{-4}	$3.37E(-5)$	1.99	$3.66E(-5)$	2.00
1×10^{-4}	$8.41E(-6)$	1.99	$9.16E(-6)$	2.00
5×10^{-5}	$2.10E(-6)$	2.00	$2.29E(-6)$	2.00
2.5×10^{-5}	$5.24E(-7)$	1.99	$5.73E(-7)$	2.00
1.25×10^{-5}	$1.31E(-7)$	2.00	$1.43E(-7)$	2.00

TABLE 1

Accuracy test: with given exact solution for the Allen-Cahn equation. The L^∞ errors at $t = 0.1$ for the phase variables ϕ computed by the scheme based on schemes BDF2 and Crank-Nicolson using **the first approach** with $G = \tanh(\frac{x}{c})$, $c = 10^4$.

δt	$BDF2 - x^3$	Order	$CN2 - x^3$	Order
8×10^{-4}	$1.47E(-3)$	–	$1.42E(-3)$	–
4×10^{-4}	$3.74E(-4)$	1.97	$3.70E(-4)$	1.94
2×10^{-4}	$9.37E(-5)$	1.99	$9.48E(-5)$	1.96
1×10^{-4}	$2.33E(-5)$	2.00	$2.39E(-5)$	1.98
5×10^{-5}	$5.84E(-6)$	1.99	$6.00E(-6)$	1.99
2.5×10^{-5}	$1.45E(-6)$	2.00	$1.50E(-6)$	2.00
1.25×10^{-5}	$3.64E(-7)$	1.99	$3.77E(-7)$	1.99

TABLE 2

Accuracy test: with given exact solution for the Allen-Cahn equation. The L^∞ errors at $t = 0.1$ for the phase variables ϕ computed by the scheme based on schemes BDF2 and Crank-Nicolson using **the first approach** with $G = x^3$.

δt	$BDF2 - \tanh(\frac{x}{c})$	Order	$CN2 - \tanh(\frac{x}{c})$	Order
8×10^{-4}	$6.39E(-5)$	–	$1.11E(-4)$	–
4×10^{-4}	$1.56E(-5)$	2.03	$2.78E(-5)$	2.00
2×10^{-4}	$3.85E(-6)$	2.02	$6.94E(-6)$	2.00
1×10^{-4}	$9.55E(-7)$	2.01	$1.73E(-6)$	2.00
5×10^{-5}	$2.38E(-7)$	2.00	$4.32E(-7)$	2.00
2.5×10^{-5}	$5.96E(-8)$	2.00	$1.08E(-7)$	2.00
1.25×10^{-5}	$1.53E(-8)$	1.96	$2.73E(-8)$	1.98

TABLE 3

Accuracy test: with given exact solution for the Allen-Cahn equation. The L^∞ errors at $t = 0.1$ for the phase variables ϕ computed by the scheme based on schemes BDF2 and Crank-Nicolson using **the second approach** with $G = \tanh(\frac{x}{c})$, $c = 10^4$.

Parameter θ is a positive constant which is associated with diffusive interface. The chemical potential for H^{-1} gradient flow is

$$(6.5) \quad \mu = \ln(1 + \phi) - \ln(1 - \phi) - \theta\phi - \epsilon^2 \Delta\phi.$$

δt	$BDF2 - x^3$	Order	$CN2 - x^3$	Order
8×10^{-4}	$6.28E(-5)$	—	$1.10E(-4)$	—
4×10^{-4}	$1.53E(-5)$	2.04	$2.77E(-5)$	1.99
2×10^{-4}	$3.77E(-6)$	2.02	$6.91E(-6)$	2.00
1×10^{-4}	$9.36E(-7)$	2.01	$1.72E(-6)$	2.00
5×10^{-5}	$2.33E(-7)$	2.01	$4.31E(-7)$	2.00
2.5×10^{-5}	$5.84E(-8)$	2.00	$1.07E(-7)$	2.01
1.25×10^{-5}	$1.50E(-8)$	1.96	$2.71E(-8)$	1.98

TABLE 4

Accuracy test: with given exact solution for the Allen-Cahn equation. The L^∞ errors at $t = 0.1$ for the phase variables ϕ computed by the scheme based on schemes BDF2 and Crank-Nicolson using the second approach with $G = x^3$.

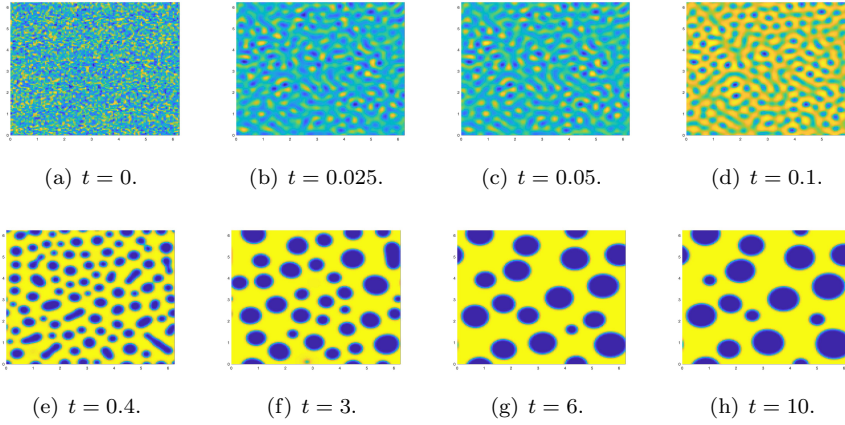


FIG. 3. Dynamical evolution of the phase variables ϕ for the Cahn-Hilliard model with logarithmic potential

We consider the second approach by choosing $G = e^{\frac{\phi}{c}}$ with $c = 10^4$ and define the new variable r as

$$(6.6) \quad r = e^{\frac{\int_{\Omega} -\frac{\theta}{2}\phi + (1+\phi)\ln(1+\phi) + (1-\phi)\ln(1-\phi) d\mathbf{x}}{c}} = G\left(\frac{\int_{\Omega} F(\phi) d\mathbf{x}}{c}\right),$$

where c is a positive constant. Compared with original SAV approach and IEQ approach, the exponential-SAV approach eliminates the constraint: $\int_{\Omega} F(\phi) d\mathbf{x} + c > 0$. In Fig. 3 we simulate the phase separation at various time by choosing phase parameters $\theta = 3$ and $\epsilon^2 = 0.002$ where initial condition is (6.1).

6.2. Molecular beam epitaxial (MBE) without slope selection. As we mentioned above, the G-SAV approach takes big advantages of dealing with the model where the nonlinear potential or free energy are unbounded from below. For example, the molecular beam epitaxial (MBE) without slope selection [32], where the total free energy is $E(\phi) = \int_{\Omega} \frac{\epsilon^2}{2} |\Delta\phi|^2 + F(\phi) dx$, and the nonlinear potential is

$$(6.7) \quad F(\phi) = -\frac{1}{2} \ln(1 + |\nabla\phi|^2).$$

Especially, the L^2 gradient flow with respect to the free energy above is

$$(6.8) \quad \phi_t = -M \frac{\delta E(\phi)}{\delta \phi} = -M(\epsilon^2 \Delta^2 \phi + F'(\phi)),$$

with periodic boundary conditions: where \mathbf{n} is the unit outward normal on the boundary $\partial\Omega$. In the above, M is a mobility constant, and $F'(\phi) = \nabla \cdot \left(\frac{\nabla \phi}{1 + |\nabla \phi|^2} \right)$.

One has to use energy splitting method [14] or stabilized method [22] to deal with the nonlinear part of energy. However, G-SAV approach can be directly applied since there is no requirement of free energy to be bounded from below. For example, we consider the tanh-SAV approach, the new variable r is set to be

$$(6.9) \quad r = \tanh\left(\frac{\int_{\Omega} -\frac{1}{2} \ln(1 + |\nabla \phi|^2) d\mathbf{x}}{c}\right) = G\left(\frac{\int_{\Omega} F(\phi) d\mathbf{x}}{c}\right),$$

where c is a positive constant. Notice that we can choose any invertible $G = x^3, x^{\frac{1}{3}}, e^{\frac{x}{c}}, \dots$, whose domain are $(-\infty, \infty)$. For example, a second-order BDF2 scheme based on the tanh-SAV approach is:

$$(6.10) \quad \frac{3\phi^{n+1} - 4\phi^n + \phi^{n-1}}{2\delta t} + M(\epsilon^2 \Delta^2 \phi^{n+1} + \frac{r^{\dagger, n}}{G(\int_{\Omega} F(\phi^{\dagger, n}) d\mathbf{x})} F'(\phi^{\dagger, n})) = 0,$$

$$(6.11) \quad \frac{3(G^{-1}(r))^{n+1} - 4(G^{-1}(r))^n + (G^{-1}(r))^{n-1}}{2\delta t} = \frac{r^{\dagger, n}}{G(\int_{\Omega} F(\phi^{\dagger, n}) d\mathbf{x})} (F'(\phi^{\dagger, n}), \frac{3\phi^{n+1} - 4\phi^n + \phi^{n-1}}{2\delta t}),$$

where $f^{\dagger, n} = 2f^n - f^{n-1}$ for any sequence $\{f^n\}$. Similarly with the proof of Theorem 2.1, we can easily show that the above equation is unconditionally energy stable. Meanwhile, the scheme (6.10)-(6.11) can also be implemented very efficiently.

We simulate the coarsening dynamical process of MBE model (6.10)-(6.11), where a random initial condition varying from -0.001 to 0.001 . The phase parameters are set to be

$$(6.12) \quad \epsilon = 0.03, \quad \delta t = 10^{-2}, \quad M = 1.$$

The computational domain is $\Omega = [0, 2\pi]^2$. The total free energy will decay with time growth where the decay rate behaves like $-88 \log(t) - 124$ which are depicted in Fig. 5. The coarse dynamic process at various time are observed in Fig. 4 which are consistent with numerical results in [14, 10].

6.3. BCP model. The (block copolymer) BCP or coupled Cahn-Hilliard system [3, 4] can be interpreted as a gradient flow as follows

$$(6.13) \quad u_t = M_u \Delta \frac{\delta E(u, v)}{\delta u},$$

$$(6.14) \quad v_t = M_v \Delta \frac{\delta E(u, v)}{\delta v},$$

with the total free energy

$$(6.15) \quad E_{\epsilon_u, \epsilon_v}(u, v) = \int_{\Omega} \frac{\epsilon_u^2}{2} |\nabla u|^2 + \frac{\epsilon_v^2}{2} |\nabla v|^2 + W(u, v) + \frac{\sigma}{2} |(-\Delta)^{-\frac{1}{2}}(v - \bar{v})|^2 d\mathbf{x},$$

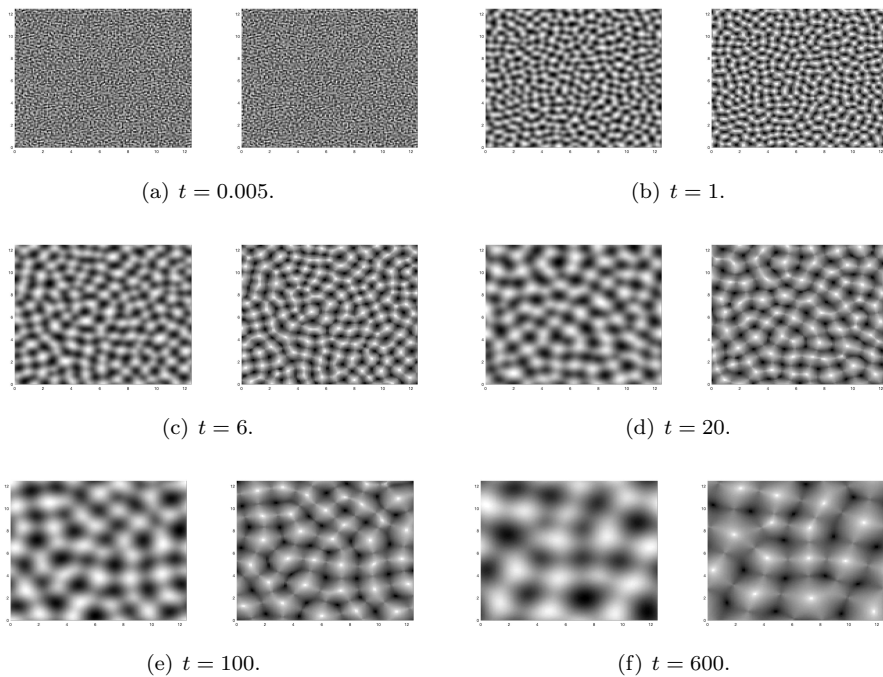


FIG. 4. The isolines of the numerical solutions of the height function ϕ and its Laplacian $\Delta\phi$ for the model without slope selection with random initial condition. For each subfigure, the left is ϕ and the right is $\Delta\phi$. Snapshots are taken at $t = 0.005, 1, 6, 20, 100, 600$, respectively.

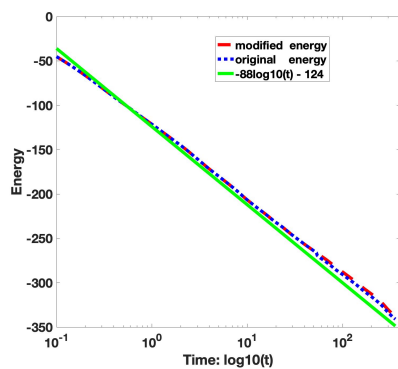


FIG. 5. The coarse dynamic evolution of energy with time for MBE model without slope selection.

where

$$W(u, v) = \frac{(u^2 - 1)^2}{4} + \frac{(v^2 - 1)^2}{4} + \alpha uv + \beta uv^2 + \gamma u^2 v.$$

Indeed, one can easily check that

$$\frac{\delta E(u, v)}{\delta u} = -\epsilon_u^2 \Delta u + \frac{\delta W}{\delta u} = \mu_u, \quad \frac{\delta E(u, v)}{\delta v} = -\epsilon_v^2 \Delta v + \frac{\delta W}{\delta v} - \sigma \Delta^{-1}(v - \bar{v}) = \mu_v.$$

The coupled Cahn-Hilliard equation describes a BCP particle is surrounded with homopolymer. The order parameter u describes these two components in the interval $[-1, 1]$, -1 represents the homopolymer rich domain and 1 is the BCP-rich domain. Order parameter v describes micro separation inside the BCP domain which also acquires values from interval $[-1, 1]$ with the end points corresponding to A-type BCP and B-type BCP. ϵ_u and ϵ_v are corresponding diffusive interface parameters and M_u and M_v are mobility constants.

Now we construct a second-order numerical scheme by using G-SAV approach and define a new variable $r = G(\int_{\Omega} W(u, v) d\mathbf{x})$ where G is a reversible function. Then the new total free energy is rewritten as

$$(6.16) \quad E_{\epsilon_u, \epsilon_v}(u, v) = \int_{\Omega} \frac{\epsilon_u^2}{2} |\nabla u|^2 + \frac{\epsilon_v^2}{2} |\nabla v|^2 + \frac{\sigma}{2} |(-\Delta)^{-\frac{1}{2}}(v - \bar{v})|^2 d\mathbf{x} + G^{-1} \{ G(\int_{\Omega} W(u, v) d\mathbf{x}) \}.$$

As in the previous section, we can construct a second-order G-SAV scheme based on BDF2 version for the above system. Assuming that u^{n-1} , u^n and v^{n-1} , v^n are known, we find u^{n+1} and v^{n+1} as follows:

$$(6.17) \quad \frac{3u^{n+1} - 4u^n + u^{n-1}}{2\delta t} = M_u \Delta \mu_u^{n+1},$$

$$(6.18) \quad \mu_u^{n+1} = -\epsilon_u^2 \Delta u^{n+1} + \left(\frac{\delta W}{\delta u}\right)^{\dagger, n} \frac{r^{n+1}}{G(\int_{\Omega} W(u^{\dagger, n}, v^{\dagger, n}) d\mathbf{x})},$$

$$(6.19) \quad \frac{3v^{n+1} - 4v^n + v^{n-1}}{2\delta t} = M_v \Delta \mu_v^{n+1},$$

$$(6.20) \quad \mu_v^{n+1} = -\epsilon_v^2 \Delta v^{n+1} + \left(\frac{\delta W}{\delta v}\right)^{\dagger, n} \frac{r^{n+1}}{G(\int_{\Omega} W(u^{\dagger, n}, v^{\dagger, n}) d\mathbf{x})}$$

$$(6.21) \quad -\sigma \Delta^{-1}(v^{n+1} - \bar{v}),$$

$$(6.21) \quad 3G^{-1}(r^{n+1}) - 4G^{-1}(r^n) + G^{-1}(r^{n-1}),$$

$$= \frac{r^{n+1}}{G(\int_{\Omega} W(u^{\dagger, n}, v^{\dagger, n}) d\mathbf{x})} \left\{ \left(\frac{\delta W}{\delta u}\right)^{\dagger, n}, 3u^{n+1} - 4u^n + u^{n-1} \right\}$$

$$+ \left(\frac{\delta W}{\delta v}\right)^{\dagger, n}, 3v^{n+1} - 4v^n + v^{n-1} \}.$$

Where $f^{\dagger, n} = 2f^n - f^{n-1}$ for any function f , and the boundary conditions are periodic. The G-SAV scheme (6.17)-(6.21) is energy stable and can be solved following the G-SAV scheme (3.7) with multi-components.

Now we make numerical experiments to simulate the annealing process [3, 4] of block copolymer and detect its morphology transformations. Phase variables for coupled Cahn-Hilliard equation are chosen as

$$(6.22) \quad \epsilon_u = 0.075 \quad \epsilon_v = 0.05 \quad \sigma = 10 \quad \alpha = 0.1 \quad \beta = -0.75 \quad \gamma = 0,$$

and domain is set to be $[-1, 1]$. The initial conditions are taken as a randomly perturbed concentration field as follows:

$$(6.23) \quad u(t=0) = \text{rand}(x, y),$$

$$(6.24) \quad v(t=0) = \text{rand}(x, y),$$

where the $\text{rand}(x, y)$ is a uniformly distributed random function in $[-1, 1]^2$ with zero mean. Assuming that the yellow bulk presents A-BCP particle and blue bulk presents

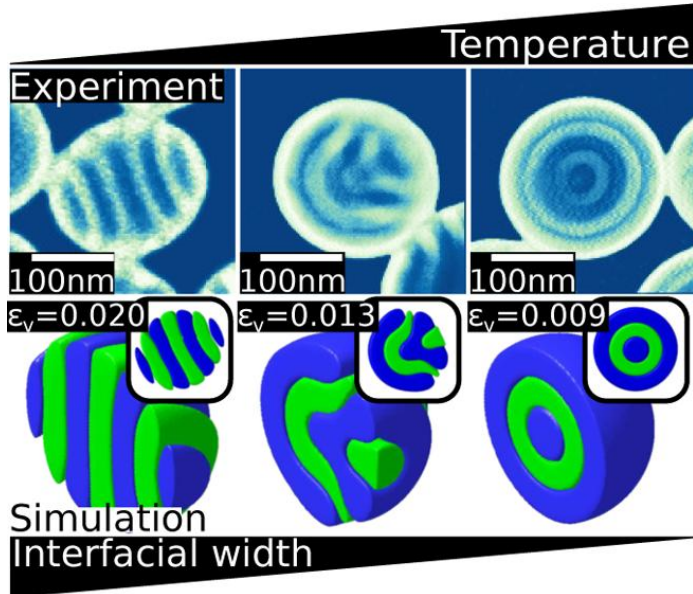


FIG. 6. *Experimental results and simulations at various temperature in [3, 4].*

as B-BCP particle. The numerical solutions in Fig. 7 and Fig. 8 are computed by G-SAV scheme (6.17)-(6.21) with $G = e^{x/c}$ and $G = \sqrt{x+c}$. From this two figures, it is observed that the contours of numerical solution are indistinguishable by using different functions G . Phase variable u presents clearly the confined surface for BCP particles. While variable v describes the dynamic process of morphological transformation for BCP particles. From Fig. 7 and Fig. 8 the striped ellipsoids gradually appears at final stage as Fig. 7. The steady morphology coincides with the experimental results depicted in Fig. 6 which also are observed in [3, 4].

7. Concluding remarks. How to construct efficient, accurate numerical schemes for gradient flows is a challenging task. The newly IEQ and SAV approaches are developed in recent years by introducing auxiliary variables. But the form of auxiliary variables can only be defined as the square root function with respect to nonlinear part of energy or nonlinear potential. We remove the definition restriction that auxiliary variables can only be square root function and develop three classes of generalized-SAV approach. Numerical schemes based on these three numerical approaches are efficient as the SAV schemes i.e., only require solving linear equations with constant coefficients at each time step. The small price to pay for the first and third approaches is to solve an additional nonlinear algebraic system which can be solved at negligible cost. For the second approach the auxiliary variable can be guaranteed to be positive by choosing tanh function or exponential function which IEQ and SAV approaches can not preserve. Moreover, all three approaches lead to schemes which are unconditionally energy stable. We present ample numerical results to show the efficiency and accuracy of numerical approaches we proposed. Our numerical results indicate that the proposed approaches can achieve accurate results which are comparable with ETDRK2 scheme and original SAV schemes. Numerical simulations from coupled Cahn-Hilliard model show that the first approach is more robust and accurate than the second approach.

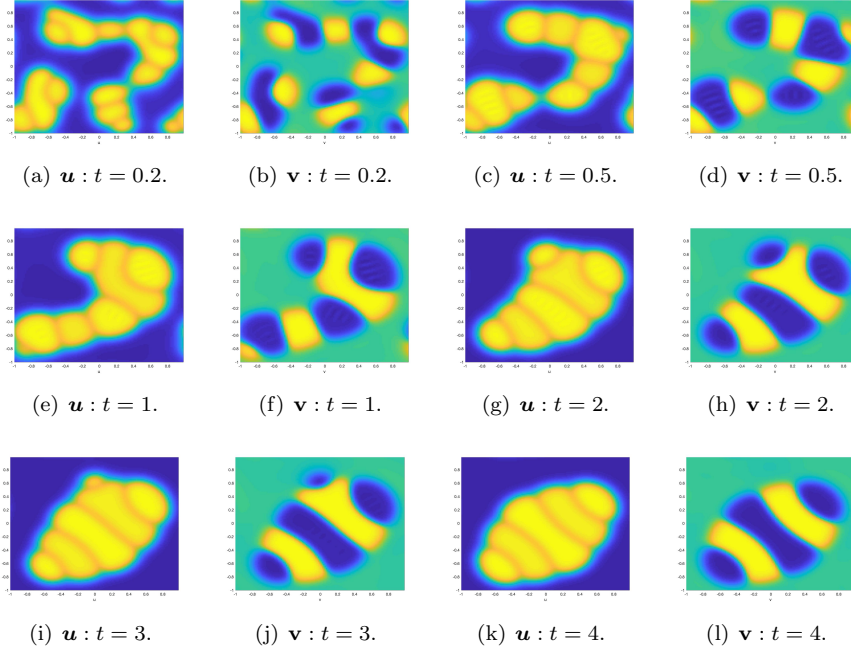


FIG. 7. The 2D dynamical evolution of the phase variable \mathbf{u}, \mathbf{v} for the Coupled-BCP model with the initial condition (6.23) and $G = e^{x/c}$ with $c = 10^4$.

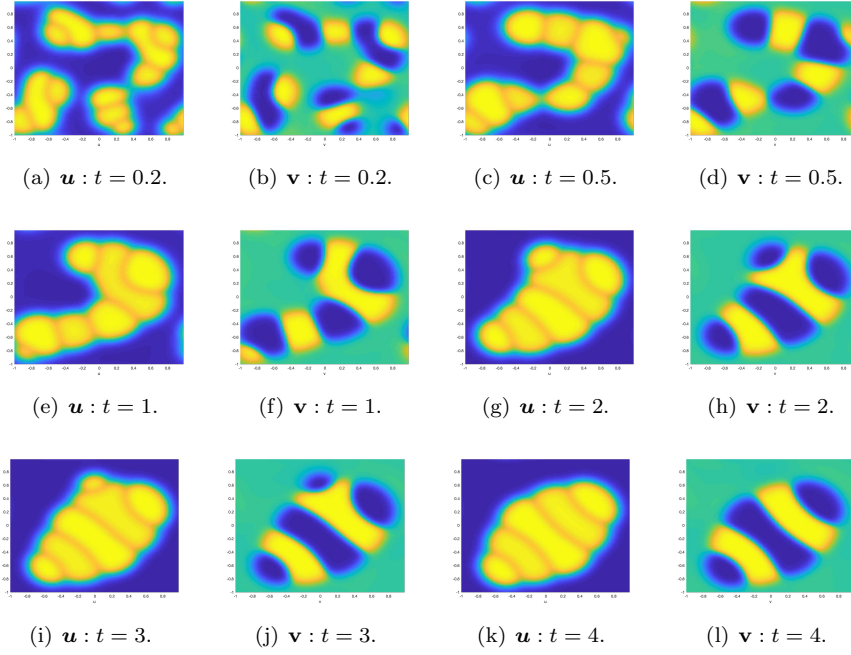


FIG. 8. The 2D dynamical evolution of the phase variable \mathbf{u}, \mathbf{v} for the Coupled-BCP model with the initial condition (6.23) and $G = \sqrt{x+c}$ with $c = 10$.

Although we consider only time-discretization schemes in this paper, they can be combined with any consistent finite dimensional Galerkin type approximations in practice, since the stability proofs are all based on variational formulations with all test functions in the same space as the trial functions.

REFERENCES

- [1] Georgios Akrivis, Buyang Li, and Dongfang li. Energy-decaying extrapolated rk–sav methods for the allen–cahn and cahn–hilliard equations. *SIAM Journal on Scientific Computing*, 41(6):A3703–A3727, 2019.
- [2] Samuel M Allen and John W Cahn. A microscopic theory for antiphase boundary motion and its application to antiphase domain coarsening. *Acta metallurgica*, 27(6):1085–1095, 1979.
- [3] Edgar Avalos, Takeshi Higuchi, Takashi Teramoto, Hiroshi Yabu, and Yasumasa Nishiura. Frustrated phases under three-dimensional confinement simulated by a set of coupled cahn–hilliard equations. *Soft matter*, 12(27):5905–5914, 2016.
- [4] Edgar Avalos, Takashi Teramoto, Hideaki Komiyama, Hiroshi Yabu, and Yasumasa Nishiura. Transformation of block copolymer nanoparticles from ellipsoids with striped lamellae into onionlike spheres and dynamical control via coupled cahn–hilliard equations. *ACS Omega*, 3(1):1304–1314, 2018.
- [5] Arvind Baskaran, John S Lowengrub, Cheng Wang, and Steven M Wise. Convergence analysis of a second order convex splitting scheme for the modified phase field crystal equation. *SIAM Journal on Numerical Analysis*, 51(5):2851–2873, 2013.
- [6] Franck Boyer and Sebastian Minjeaud. Numerical schemes for a three component cahn–hilliard model. *ESAIM: Mathematical Modelling and Numerical Analysis*, 45(4):697–738, 2011.
- [7] John W Cahn and John E Hilliard. Free energy of a nonuniform system. i. interfacial free energy. *The Journal of chemical physics*, 28(2):258–267, 1958.
- [8] John W Cahn and John E Hilliard. Free energy of a nonuniform system. iii. nucleation in a two-component incompressible fluid. *The Journal of chemical physics*, 31(3):688–699, 1959.
- [9] Elena Celledoni, Volker Grimm, Robert I McLachlan, DI McLaren, D O’Neale, Brynjulf Owren, and GRW Quispel. Preserving energy resp. dissipation in numerical pdes using the average vector field method. *Journal of Computational Physics*, 231(20):6770–6789, 2012.
- [10] Wenbin Chen, Cheng Wang, Xiaoming Wang, and Steven M Wise. A linear iteration algorithm for a second-order energy stable scheme for a thin film model without slope selection. *Journal of Scientific Computing*, 59(3):574–601, 2014.
- [11] Wenbin Chen, Cheng Wang, Xiaoming Wang, and Steven M Wise. Positivity-preserving, energy stable numerical schemes for the cahn–hilliard equation with logarithmic potential. *Journal of Computational Physics: X*, 3:100031, 2019.
- [12] Qing Cheng, Chun Liu, and Jie Shen. A new lagrange multiplier approach for gradient flows. November 2019.
- [13] Qing Cheng and Jie Shen. Multiple scalar auxiliary variable (msav) approach and its application to the phase-field vesicle membrane model. *SIAM Journal on Scientific Computing*, 40(6):A3982–A4006, November 2018.
- [14] Qing Cheng, Jie Shen, and Xiaofeng Yang. Highly efficient and accurate numerical schemes for the epitaxial thin film growth models by using the sav approach. *Journal of Scientific Computing*, 78(3):1467–1487, 2019.
- [15] Laurence Cherfils, Alain Miranville, and Sergey Zelik. The cahn–hilliard equation with logarithmic potentials. *Milan Journal of Mathematics*, 79(2):561–596, 2011.
- [16] Steven M Cox and Paul C Matthews. Exponential time differencing for stiff systems. *Journal of Computational Physics*, 176(2):430–455, 2002.
- [17] Qiang Du and Xiaobing Feng. The phase field method for geometric moving interfaces and their numerical approximations. *arXiv preprint arXiv:1902.04924*, 2019.
- [18] Qiang Du, Lili Ju, Xiao Li, and Zhonghua Qiao. Stabilized linear semi-implicit schemes for the nonlocal cahn–hilliard equation. *Journal of Computational Physics*, 363:39–54, 2018.
- [19] Charles M Elliott and AM Stuart. The global dynamics of discrete semilinear parabolic equations. *SIAM journal on numerical analysis*, 30(6):1622–1663, 1993.
- [20] David J Eyre. Unconditionally gradient stable time marching the cahn–hilliard equation. *MRS online proceedings library archive*, 529, 1998.
- [21] Francisco Guillén-González and Giordano Tierra. On linear schemes for a cahn–hilliard diffuse interface model. *Journal of Computational Physics*, 234:140–171, 2013.
- [22] Dianming Hou, Mejdi Azaiez, and Chuanju Xu. A variant of scalar auxiliary variable approaches

- for gradient flows. *Journal of Computational Physics*, 2019.
- [23] Haydi Israel. Long time behavior of an allen-cahn type equation with a singular potential and dynamic boundary conditions. *J. Appl. Anal. Comput*, 2(1):29–56, 2012.
- [24] Xiaobo Jing, Jun Li, Xueping Zhao, and Qi Wang. Second order linear energy stable schemes for allen-cahn equations with nonlocal constraints. *Journal of Scientific Computing*, 80(1):500–537, 2019.
- [25] Dong Li, Zhonghua Qiao, and Tao Tang. Characterizing the stabilization size for semi-implicit fourier-spectral method to phase field equations. *SIAM Journal on Numerical Analysis*, 54(3):1653–1681, 2016.
- [26] Zhengguang Liu and Xiaoli Li. The exponential scalar auxiliary variable (e-sav) approach for phase field models and its explicit computing. *arXiv preprint arXiv:1912.09263*, 2019.
- [27] Zhonghua Qiao, Zhi-zhong Sun, and Zhengru Zhang. The stability and convergence of two linearized finite difference schemes for the nonlinear epitaxial growth model. *Numerical Methods for Partial Differential Equations*, 28(6):1893–1915, 2012.
- [28] GRW Quispel and David Ian McLaren. A new class of energy-preserving numerical integration methods. *Journal of Physics A: Mathematical and Theoretical*, 41(4):045206, 2008.
- [29] Jie Shen, Jie Xu, and Jiang Yang. The scalar auxiliary variable (sav) approach for gradient flows. *Journal of Computational Physics*, 353:407–416, 2018.
- [30] Jie Shen, Jie Xu, and Jiang Yang. A new class of efficient and robust energy stable schemes for gradient flows. *SIAM Review*, 61(3):474–506, July 2019.
- [31] Jie Shen and Xiaofeng Yang. The ieq and sav approaches and their extensions for a class of highly nonlinear gradient flow systems. In *Celebrating 75 Years of Mathematics of Computation*.
- [32] J Villain. Continuum models of crystal growth from atomic beams with and without desorption. *Journal de physique I*, 1(1):19–42, 1991.
- [33] Xiaofeng Yang. Linear, first and second-order, unconditionally energy stable numerical schemes for the phase field model of homopolymer blends. *Journal of Computational Physics*, 327, December 2016.
- [34] Xiaofeng Yang, Jia Zhao, Qi Wang, and Jie Shen. Numerical approximations for a three-component cahn–hilliard phase-field model based on the invariant energy quadratization method. *Mathematical Models and Methods in Applied Sciences*, 27(11):1993–2030, 2017.
- [35] Xiaofeng Yang, Jia Zhao, Qi Wang, and Jie Shen. Numerical approximations for a three components Cahn-Hilliard phase-field model based on the invariant energy quadratization method. *M3AS: Mathematical Models and Methods in Applied Sciences*, 27(11), August 2017.
- [36] Yang Zhiguo and Dong Suchuan. A roadmap for discretely energy-stable schemes for dissipative systems based on a generalized auxiliary variable with guaranteed positivity. *Journal of Computational Physics*, 404, 2020.